MOX-Report No. 04/2025

Nonlinear morphoelastic theory of biological shallow shells with initial stress

Andrini, D.; Magri, M.; Ciarletta, P.

MOX, Dipartimento di Matematica
Politecnico di Milano, Via Bonardi 9 - 20133 Milano (Italy)

mox-dmat@polimi.it https://mox.polimi.it

Nonlinear morphoelastic theory of biological shallow shells with initial stress

D. Andrini[1], X. Chen[2], P. Ciarletta[1*]

[1] MOX, Dipartimento di Matematica, Politecnico di Milano, piazza Leonardo da Vinci 32, 20133 Milano, Italy,

[2] Guangdong Provincial Key Laboratory of Interdisciplinary Research and Application for Data Science, BNU-HKBU United International College, Zhuhai, 519087, China.

Abstract

Shallow shells are widely encountered in biological structures, especially during embryogenesis, when they undergo significant shape variations. As a consequence of geometric frustration caused by underlying biological processes of growth and remodeling, such thin and moderately curved biological structures experience initial stress even in the absence of an imposed deformation. In this work, we perform a rigorous asymptotic expansion from three-dimensional elasticitiy to obtain a nonlinear morphoelastic theory for shallow shells accounting for both initial stress and large displacements. By application of the principle of stationary energy for admissible variation of the tangent and normal displacement fields with respect to the reference middle surface, we derive two generalised nonlinear equilibrium equations

[*]Corresponding author. E-mail: pasquale.ciarletta@polimi.it

of the Marguerre-von Kármán type. We illustrate how initial stress distributions drive the emergence of spontaneous mean and Gaussian curvatures which are generally not compatible with the existence of a stress free configuration. We also show how such spontaneous curvatures influence the structural behavior in the solutions of two systems: a saddle-like and a cylindrical shallow shell.

Keywords: Elastic shallow shell, Marguerre-von Kármán equations, residual stress, asymptotic theory.

1 Introduction

Shallow shells are characterized by their moderately curved, thin-walled geometry and are found in numerous biological structures such as blood vessels, cell membranes, and plant tissues [1]. In the biological realm, they are also widely encountered in early stages of embryos in the form of curved monolayers or cell sheets undergoing folding and shaping under the action of physical forces [21].

In continuum mechanics, the fundamental concepts for the linear elastic theory of shallow shells was proposed by Marguerre [24] under the assumptions of small strains and rotations. Reissner later expanded the theory by considering the effects of transverse shear deformation, which was particularly important for thick shells [34], making the models more applicable to a wider range of engineering problems.

Since living matter undergoes significant deformations during processes such as cell migration and division, nonlinear models are needed to describe their mechanics accurately [16]. Nonlinear shallow shells models indeed account for large strains and rotations, being capable of capturing post-buckling behavior, large deflections, and more complex stability phenomena [33, 27].

Notable contributions were made by Novozhilov who developed a theory for thin shells with geometric nonlinearities [32], and by Naghdi who provided a robust mathematical framework for analyzing the stability and dynamic response of shallow shells [20, 28], including the effects of initial imperfections and nonlinear material properties [26].

A comprehensive review of rigorous mathematical derivations of both linear and nonlinear models for elastic shallow shells from three-dimensional elasticity was given by Ciarlet [7], together with other notable works on the existence and uniqueness of solutions to nonlinear shell theories [8], the development of higher-order shell models [6], and the derivations of intrinsic equation, whose sole unknowns are the bending moments and the stress resultants [9]. More recent contributions also provided crucial insights into the stability and post-buckling behavior of shallow shells [37, 36], also from a computational viewpoint [5].

The use of asymptotic shell and shallow shell models for biological materials has been extensively explored. In a seminal work, Helfrish et al. [17] extended classical shell theories to account for the anisotropic behavior of biological membranes, shedding light on the mechanical response of lipid bilayers to external stimuli. A refined theoretical framework for analyzing the growth and form of thin elastic sheets was later proposed for highlighting the role of geometric constraints in shaping biological structures [12], with applications to the mechanics of cellular membranes to investigate the interplay between membrane curvature and mechanical properties [13]. These mechanical models revived the interest in shallow shell theories for the morphogenesis of biological tissues, revealing how tissue folding arises from mechanical instabilities [3].

An accurate analysis of biological shell structures requires to consider a pre-stressed configuration accounting for initial or residual stresses, which are ubiquitous in biological materials. Initial stresses often emerge due to differential growth or remodeling, playing a pivotal role in driving morphogenetic processes and influencing the stability of biological structures [38, 2, 14]. These effects are particularly relevant during embryogenesis, where growth-induced residual stresses are responsible for complex tissue folding and the emergence of functional shapes, even in the absence of traction loads [30, 39, 41]. Residual stresses significantly influence mechanical responses, such as arterial wall thickening or tumor-induced deformations [19, 4]. A rigorous understanding of the coupling between growth, remodeling, and initial stress is therefore crucial for addressing key biological questions and developing predictive models for the morphogenesis of biological shells. Previous studies have highlighted the importance of residual stresses in biological structures, demonstrating their influence on deformation [31]. They also explore the role of residual stresses in the mechanical behavior of arterial walls, emphasizing their impact on structural stability and pathology [42], and in marine organisms to emphasize evolutionary adaptation and structural optimization [29]. Extending classical shallow shell models to include these factors is crucial for more accurate prediction of structural behaviors.

In the following, we present a formal asymptotic derivation of the nonlinear shallow shell equations for an elastic shell with initial stresses. In Section 2, we introduce the geometric and kinematical framework as well as the constitutive theory of nonlinear elastic shells with initial stresses under the assumption of material isotropy. In Section 3, we introduce the scaling assumptions for the geometrical parameters and the initial stress, and we derive by means of a dimensional reduction procedure, the governing equations for an initially stressed elastic shallow shell. In Section 4, we explicitly solve the derived shallow shell equations in two physical system models, discussing how the initial stress concentration may drive the emergence of spontaneous curvatures and buckling patterns. Concluding remarks are finally summarized in Section 5.

2 The nonlinear three-dimensional elastic model

In this section, we derive the three-dimensional nonlinear theory for biological elastic shells with initial stress. Classical approaches to nonlinear shell theory rigorously derive governing equations under the assumption of a stress-free reference configuration. Our derivation builds upon this foundation by explicitly incorporating initial stresses into the three-dimensional elastic potential. This inclusion allows us to capture the effects of strain incompatibilities that are prevalent in morphoelastic systems, providing a more general framework. This approach aligns with related studies on incompatible strains, such as the works [22, 10] for plates. By extending these concepts to shallow shells, we introduce a methodology to analyze how residual stresses influence nonlinear morphologies and stability, particularly in contexts where geometric frustration drives spontaneous curvature and buckling. In the following, we first detail the kinematic and geometric assumptions pertaining to shells and then discuss the constitutive theory accounting for initial stress.

2.1 Geometric and kinematic assumptions

Let us consider an incompressible nonlinear shell with reference configuration $\mathcal{B}_{\boldsymbol{\tau}}$, occupying the region consisting of all points within a distance $H << 1$ from a given reference middle surface ω_τ embedded in the three-dimensional Euclidean space $\mathbb{E}^3$. In the following, we will consider that $\mathcal{B}_{\boldsymbol{\tau}}$ is an initially stressed configuration that is characterized by a given initial distribution of the Cauchy stress tensor τ. The *initial* stresses will be referred to as *residual* stresses, when the entire boundary $\partial\mathcal{B}_{\boldsymbol{\tau}}$ is taken free of traction loads. We assume that the surface ω_τ can be parameterized by a smooth injective mapping from the parameter space $\mathcal{P} \subset \mathbb{R}^2$ to the Euclidean space $\mathbb{E}^3$. In the following, Greek letters range over 1 and 2, while Latin letters range from 1 to 3. Moreover, repeated summation convention is employed over dummy indices and subscript comma denotes differentiation with respect to the following variable. Accordingly, the material position of each point $\boldsymbol{X}_0 \in \omega_\tau$ is given by $\boldsymbol{X}_0 = \boldsymbol{X}_0(\Theta^\alpha)$, where $\Theta^\alpha \in \mathcal{P}$ are the reference curvilinear coordinates (see figure 1). Consequently, the covariant coordinate vectors that are tangent to the reference middle surface are given by:

$$\boldsymbol{G}_1 = \frac{\partial \boldsymbol{X}_0}{\partial \Theta^1}, \quad \boldsymbol{G}_2 = \frac{\partial \boldsymbol{X}_0}{\partial \Theta^2}. \tag{1}$$

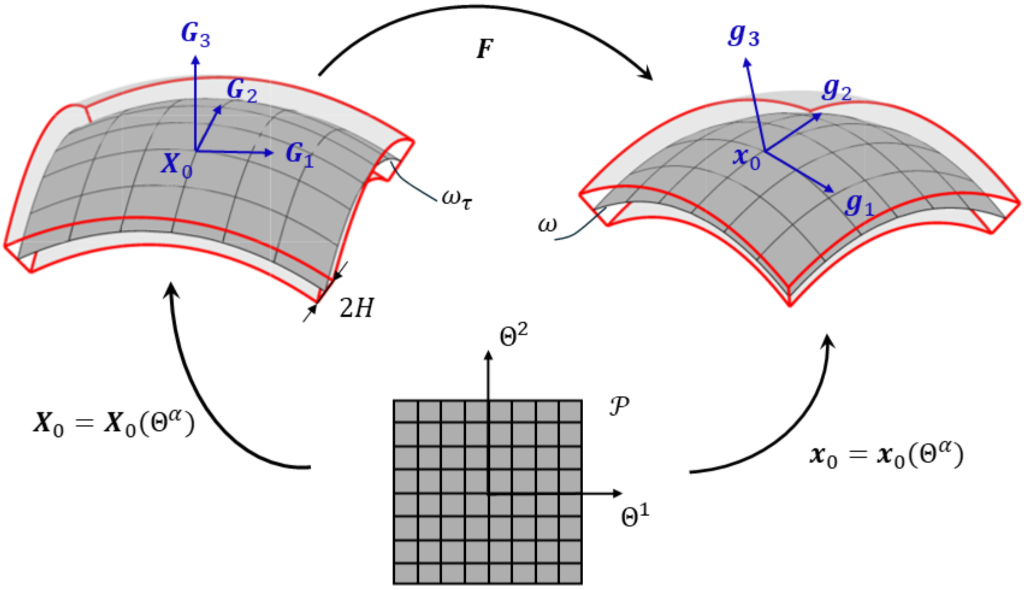

Figure 1: Sketch of the reference and spatial configuration of the shell, with indication of the middle surface (shaded grey). We also depict the covariant bases $\boldsymbol{G}_i$, $\boldsymbol{g}_i$ at the reference $\boldsymbol{X}$, and spatial $\boldsymbol{x}$ position of the middle surface ω_τ and ω, respectively.

We then define the corresponding contravariant basis $\boldsymbol{G}^\alpha$ so that $\boldsymbol{G}_\alpha \cdot \boldsymbol{G}^\beta = \delta_\alpha^\beta$, δ_α^β being the Kronecker delta. The six independent scalar products $G_{\alpha\beta} = \boldsymbol{G}_\alpha \cdot \boldsymbol{G}_\beta$ and $G^{\alpha\beta} = \boldsymbol{G}^\alpha \cdot \boldsymbol{G}^\beta$ represent the covariant and contravariant components of the metric tensor on the reference middle surface, respectively. We then indicate with $\boldsymbol{G}_3$ the unit vector normal to the mid-surface ω_τ, which we assume to be continuously varying throughout the domain. It is defined as:

$$\boldsymbol{G}_3 = \boldsymbol{G}^3 = \frac{\boldsymbol{G}_1 \wedge \boldsymbol{G}_2}{|\boldsymbol{G}_1 \wedge \boldsymbol{G}_2|}. \tag{2}$$

Finally, using the Weingarten formulas, the curvature tensor of the reference middle surface is given by:

$$\mathsf{K} = -\frac{\partial \boldsymbol{G}_3}{\partial \Theta^\alpha} \otimes \boldsymbol{G}^\alpha, \tag{3}$$

where $\otimes$ denotes the dyadic product, and $\mathcal{H} = \mathrm{tr}(\mathsf{K})/2$ and $\mathcal{K} = \det(\mathsf{K})$ are the referential mean and Gaussian curvatures, respectively.

For the subsequent analysis it is useful to be more specific about the coordinate system that we adopt to describe the three-dimensional region occupied by the shell, $\mathcal{B}_\tau$. We can define such coordinates starting from the ones used for the mid-surface and express the material position $\boldsymbol{X} \in \mathcal{B}_\tau$ as follows

$$\boldsymbol{X}(\Theta^1, \Theta^2, \zeta) = \boldsymbol{X}_0(\Theta^1, \Theta^2) + \zeta\, \boldsymbol{G}_3(\Theta^1, \Theta^2), \tag{4}$$

with $\zeta \in [-H, H]$. In such a way, $\mathcal{B}_{\boldsymbol{\tau}}$ is the corresponding image of $\mathcal{P} \times [-H, H]$, and $(\Theta^1, \Theta^2, \zeta)$ are the natural curvilinear coordinates of the shell in the reference configuration. Consequently, we can also define the covariant $\bar{\boldsymbol{G}}_\alpha$ and contravariant $\bar{\boldsymbol{G}}^\alpha$ basis vectors at an arbitrary point *within* $\mathcal{B}_\tau$, and not just on the mid surface. It is easy to calculate them by differentiating Eq.(4) and exploiting Eq.(3). They are given by:

$$\bar{\boldsymbol{G}}_\alpha = \frac{\partial \boldsymbol{X}}{\partial \Theta^\alpha} = (1 - \zeta\mathsf{K})\boldsymbol{G}_\alpha, \quad \bar{\boldsymbol{G}}^\alpha = (1 - \zeta\mathsf{K})^{-T}\boldsymbol{G}^\alpha. \tag{5}$$

We remark that they are still orthogonal to the unit normal $\boldsymbol{G}_3$, similarly to their counterpart on the mid surface.

Finally, again by differentiation of Eq.(4), the area and volume elements on the reference shell read:

$$\begin{aligned} \mathrm{d}A &= |\boldsymbol{G}_1 \wedge \boldsymbol{G}_2|\, \mathrm{d}\Theta = G\, \mathrm{d}\Theta, \\ \mathrm{d}V &= \det(\mathsf{I}_2 - \zeta\mathsf{K})\, \mathrm{d}\Theta\, \mathrm{d}\zeta = (1 - 2\zeta\mathcal{H} + \zeta^2\mathcal{K})\ \mathrm{d}\Theta\, \mathrm{d}\zeta, \end{aligned} \tag{6}$$

where $\mathrm{d}\Theta = \mathrm{d}\Theta^1\, \mathrm{d}\Theta^2$, G is the determinant of the metric tensor, i.e. $G = \det G_{\alpha\beta}$, and I_2 is the rank-2 unit tensor in the space tangent to the shell.

After deformation, the spatial position of a point $\boldsymbol{x}$ within the current configuration $\mathcal{B}$ of the shell is also expressed by a one-to-one function of the natural curvilinear coordinates, namely

$$(\Theta_1, \Theta_2, \zeta) \mapsto \boldsymbol{x}(\Theta^1, \Theta^2, \zeta) \in \mathcal{B}. \tag{7}$$

The deformed middle surface is then mapped by $\boldsymbol{x}_0 = \boldsymbol{x}(\Theta^1, \Theta^2, 0)$ as reported in the commutative diagram in Fig.1. Hence, the tangent plane of the deformed middle surface is spanned by the covariant and contravariant coordinate vectors defined as:

$$\boldsymbol{g}_\alpha = (\boldsymbol{x}_0)_{,\alpha}, \qquad \boldsymbol{g}_\alpha \cdot \boldsymbol{g}^\beta = \delta_\alpha^\beta. \tag{8}$$

The above formulas define the six independent scalar products $g_{\alpha\beta} = \boldsymbol{g}_\alpha \cdot \boldsymbol{g}_\beta$ and $g^{\alpha\beta} = \boldsymbol{g}^\alpha \cdot \boldsymbol{g}^\beta$ representing the covariant and contravariant components of the metric tensor on the deformed middle surface. Accordingly, the deformation gradient from the reference to the spatial configuration of the shell is given by:

$$\mathsf{F} = \frac{\partial \boldsymbol{x}}{\partial \boldsymbol{X}} = \boldsymbol{x}_{,\alpha} \otimes \bar{\boldsymbol{G}}^\alpha + \frac{\partial \boldsymbol{x}}{\partial \zeta} \otimes \boldsymbol{G}^3. \tag{9}$$

Finally, dealing with biological materials, we also assume that the mapping is volume preserving and so we impose the incompressibility constraint:

$$J - 1 = 0, \tag{10}$$

where J denotes the Jacobian of the deformation gradient, namely, $J := \det \mathsf{F}$.

2.2 Constitutive theory with initial stresses

The reference configuration of living matter often possesses initial stresses, arising from the presence of either geometric misfit or differential growth processes during their development. We denote by $\boldsymbol{\tau} = \boldsymbol{\tau}(\boldsymbol{X})$ the Cauchy stress tensor in the reference configuration of the shell. Since the reference configuration is equilibrated, it must obey the following balance equation:

$$\mathrm{Div}\,\boldsymbol{\tau} = \bar{\boldsymbol{G}}^{\alpha} \cdot \tau_{,\alpha} + \boldsymbol{G}^3 \cdot \frac{\partial \tau}{\partial \zeta} = \mathbf{0}, \qquad \tau = \tau^T \qquad \text{in} \quad \mathcal{B}_\tau, \tag{11}$$

where Div is the material divergence operator in the material configuration. Notice that, for *residual stresses*, the entire boundary $\partial\mathcal{B}_{\boldsymbol{\tau}}$ is free of traction. Hence, in that case we also impose $\boldsymbol{\tau}\boldsymbol{N} = \mathbf{0}$, with $\boldsymbol{N}$ being the local unit normal in the material boundary. In such a case, by simple application of the mean value theorem, the stress τ is inhomogeneous and has a zero average over in $\mathcal{B}_\tau$ [18].

We assume a perfectly elastic consitutive response of the body from the residually stressed initial configuration, and define a strain energy density Ψ per unit reference volume that explicitly depends on both the deformation gradient and the residual stress tensor:

$$\Psi(\boldsymbol{X}) = \bar{\Psi}(\mathsf{F}(\boldsymbol{X}), \tau(\boldsymbol{X})). \tag{12}$$

By usual invariance requirements under rigid-body motion, the strain energy can be expressed as a function of the three invariants of the right Cauchy-Green tensor $\mathsf{C} = \mathsf{F}^T\mathsf{F}$, the three invariants of the initial stress tensor τ, plus their four mixed invariants [35, 25]. Accordingly, the presence of the residual stress adds inhomogeneity to the material response and changes the symmetry group of the material response relative to the reference configuration. Following standard thermo-mechanical arguments for isochoric deformations, the first and second Piola-Kirchhoff stress tensors, P and S, are respectively given by:

$$\mathsf{P} = \frac{\partial \bar{\Psi}}{\partial \mathsf{F}}(\mathsf{F}, \tau) - pJ\mathsf{F}^{-1}, \qquad \mathsf{S} = \frac{\partial \bar{\Psi}}{\partial \mathsf{F}}(\mathsf{F}, \tau)\mathsf{F}^{-T} - pJ\mathsf{C}^{-1}, \tag{13}$$

where p is the Lagrange multiplier enforcing the incompressibility constraint.

Aiming to develop a shallow shell theory accounting for geometric nonlinearities, we consider the constitutive response of a residually stressed neo-Hookean material, given by

[15]:

$$\bar{\Psi}(\mathsf{F}, \tau) = \tilde{\Psi}(\operatorname{tr}\mathsf{C}, \operatorname{tr}(\tau\mathsf{C}), I_{\tau 1}, I_{\tau 2}, I_{\tau 3}) = \frac{1}{2}\left(\operatorname{tr}(\tau\mathsf{C}) + r\operatorname{tr}\mathsf{C} - 3\mu\right), \tag{14}$$

where μ is the shear modulus of the unstressed material, $I_{\tau 1} = \operatorname{tr}\tau$, $I_{\tau 2} = \frac{1}{2}[(I_{\tau 1}^2 - \operatorname{tr}(\tau^2)]$, $I_{\tau 3} = \det\tau$, and $r = r(I_{\tau 1}, I_{\tau 2}, I_{\tau 3})$ is the real root of:

$$r^3 + I_{\tau 1}r^2 + I_{\tau 2}r + I_{\tau 3} - \mu^3 = 0. \tag{15}$$

We remark that the actual Cauchy stress σ must equal the initial stress tensor τ in the absence of deformation. Hence, being $\sigma(\mathsf{F}) = J\mathsf{F}\mathsf{P}$, we immediately deduce:

$$\tau = \sigma(\mathsf{I}) = \frac{\partial\Psi}{\partial\mathsf{F}}(\mathsf{I}, \tau) - p_\tau\mathsf{I}, \qquad p_{\boldsymbol{\tau}} = r. \tag{16}$$

From (13), the constitutive equation for the initially stressed Neo-Hookean material with strain energy given by (14) is:

$$\mathsf{P} = r\mathsf{F}^T - pJ\mathsf{F}^{-1} + \tau\mathsf{F}^T, \qquad \mathsf{S} = r\mathsf{I} - pJ\mathsf{C}^{-1} + \tau. \tag{17}$$

We finally recall that, if we neglect the presence of body forces, the equilibrium conditions in the reference configuration are:

$$\operatorname{Div}\mathsf{P} = \mathbf{0}, \qquad \mathsf{F}\,\mathsf{P} = \mathsf{P}^T\mathsf{F}^T \qquad \text{in} \quad \mathcal{B}_\tau, \tag{18}$$

together with the traction boundary conditions $\boldsymbol{N}\mathsf{P} = \boldsymbol{l}$ on $\partial\mathcal{B}_\tau$, $\boldsymbol{l}$ being the surface tractions.

3 Variational formulation of a nonlinear theory of initially stressed shallow shells

In this Section we introduce the *shallow shell assumptions* and subsequently derive the reduced nonlinear theory by means of a variational asymptotic procedure.

3.1 Shallowness of the reference configuration

We preliminary remark that, the shell domain $\mathcal{B}_\tau$ features two main characteristic lengths, L being the geodetic diameter of the set ω_τ and H, the half-thickness of the shell. The latter is supposed to be small with respect to L and so we can identify a small dimensionless parameter $\epsilon = H/L \ll 1$.

Let us then introduce the Cartesian unit vectors $(\boldsymbol{E}_1, \boldsymbol{E}_2, \boldsymbol{E}_3)$ in the reference configuration and parametrize the reference position of the middle surface ω_τ by:

$$\boldsymbol{X}_0(\Theta^1, \Theta^2) = \Theta^1\,\boldsymbol{E}_1 + \Theta^2\,\boldsymbol{E}_2 + Z(\Theta^1, \Theta^2)\,\boldsymbol{E}_3. \tag{19}$$

According to the above formula, the *shallowness assumptions* imposes that in every point of the spatial domain of the shell, the following holds:

$$\max|Z_{,\alpha}| \ll 1. \tag{20}$$

In particular, for the purpose of the subsequent dimensional reduction, we will assume a specific scaling of the slope of the shell, namely, $Z_{,\alpha} = O(\epsilon)$ uniformly throughout the domain.

Given the parametrization in Eq (19), the covariant base reads:

$$\boldsymbol{G}_\alpha = \boldsymbol{E}_\alpha + Z_{,\alpha}\boldsymbol{E}_3, \tag{21}$$

and, accordingly, the covariant metric components are $G_{\alpha\beta} = \delta_{\alpha\beta} + Z_{,\alpha} Z_{,\beta}$, so that at the leading order, the coordinate lines are orthogonal everywhere and the metric is *flat*. Similarly, the unit normal vector of the middle surface can be approximated as $\boldsymbol{G}_3 = -Z_{,\alpha} \boldsymbol{E}_\alpha + \boldsymbol{E}_3 + o(\epsilon^2)$, and the mean and Gaussian curvature at the *leading order* read, respectively:

$$\mathcal{H} = \frac{Z_{,\alpha\alpha}}{2}, \qquad \mathcal{K} = Z_{,11} Z_{,22} - Z_{,12}^2 = [Z, Z], \tag{22}$$

where with the square brackets we denote the following bilinear operator $[a, b] = 1/2(a_{,11} b_{,22} + b_{,11} a_{,22} - 2a_{,12} b_{,12})$. We also remark that, at the leading order, the surface coordinates are lines of curvature coordinate if and only if $Z_{,12} = 0$.

It is important to mention that, to be consistent with the shallowness hypothesis, the shell is supposed to remain shallow even *after the deformation*. Hence it is essential to derive proper scaling laws for the tangent and normal displacements. This issue will be addressed in the next Subsection.

3.2 Scaling for the displacement fields

We expand the spatial position of any point within the shell as follows

$$\boldsymbol{x}(\Theta^\alpha, \zeta) = \boldsymbol{X}(\Theta^\alpha, \zeta) + \boldsymbol{u}_0(\Theta^\alpha) + \zeta \boldsymbol{u}_1(\Theta^\alpha) + o(\epsilon^3 L), \tag{23}$$

where $\boldsymbol{u}_0(\Theta^\alpha)$ is the displacement of the middle surface. Following standard arguments, we formulate two other *shallow shell assumptions*: one for the displacement of the middle surface and another for the rotation vectors. Using (21) and (20), we first assume that the planar components of the displacement fields are much smaller then the normal components. In particular, we set

$$\boldsymbol{u}_0(\Theta^\alpha) = U_\alpha(\Theta^\alpha) \, \boldsymbol{E}^\alpha + W(\Theta^\alpha) \, \boldsymbol{E}_3, \quad \boldsymbol{u}_1(\Theta^\alpha) = U_{\zeta\alpha}(\Theta^\alpha) \, \boldsymbol{E}_\alpha + W_\zeta(\Theta^\alpha) \, \boldsymbol{E}_3, \tag{24}$$

with $U_\alpha = O(\epsilon^2 L)$ and $W = O(\epsilon L)$. To set the order of magnitude of $\boldsymbol{u}_1$ we argue as follows: we define the rotation vectors as $\boldsymbol{\eta}_\alpha = \boldsymbol{G}_\alpha \wedge \mathsf{F}\boldsymbol{G}_\alpha$ and assume that their component along the normal direction are much smaller than their planar counterparts, so that:

$$\boldsymbol{\eta}_\alpha \cdot \boldsymbol{G}_\beta = O(\epsilon), \text{ for } \alpha \neq \beta, \qquad \boldsymbol{\eta}_\alpha \cdot \boldsymbol{G}_3 = O(\epsilon^2). \tag{25}$$

Hence, the rotation around the normal is much smaller than the rotation around any axis in the tangential plane of the middle surface. By combining (24) and (25), we deduce the following scaling: $U_{\zeta\alpha} = O(\epsilon)$ and $W_\zeta = O(\epsilon^2)$.

It is now possible to compute an approximation of the Cauchy-Green strain tensor C. By using Eq.(9), it is easy to deduce:

$$\mathsf{C} = \mathsf{F}^T\mathsf{F} = (\boldsymbol{x}_{,\alpha} \cdot \boldsymbol{x}_{,\beta})\bar{\boldsymbol{G}}^\beta \otimes \bar{\boldsymbol{G}}^\alpha + |\boldsymbol{G}_3 + \boldsymbol{u}_1|^2 \boldsymbol{G}^3 \otimes \boldsymbol{G}^3, \tag{26}$$

which, neglecting terms of order $o(\epsilon^2)$, can be expanded as:

$$\mathsf{C} = \mathsf{I} + \mathsf{A}_0 + \zeta\, \mathsf{A}_\zeta, \tag{27}$$

with:

$$\mathsf{A}_0 = (U_{\alpha,\beta} + U_{\beta,\alpha} + W_{,\alpha}W_{,\beta} - U_{\zeta\alpha}Z_{,\beta} - U_{\zeta\beta}Z_{,\alpha})\boldsymbol{E}_\alpha \otimes \boldsymbol{E}_\beta + \tag{28}$$

$$+(U_{\zeta\alpha} + W_{,\alpha})(\boldsymbol{E}_3 \otimes \boldsymbol{E}_\alpha + \boldsymbol{E}_\alpha \otimes \boldsymbol{E}_3) + \tag{29}$$

$$+(2W_\zeta + U^2_{\zeta,\alpha} + 2W_{,\alpha}Z_{,\alpha})\boldsymbol{E}_3 \otimes \boldsymbol{E}_3 = O(\epsilon^2), \tag{30}$$

$$\mathsf{A}_\zeta = (U_{\zeta\alpha,\beta} + U_{\zeta\beta,\alpha})\boldsymbol{E}_\alpha \otimes \boldsymbol{E}_\beta = O(\epsilon/L). \tag{31}$$

For later purposes it is worth mentioning two more consequences of the kinematic assumptions expressed in (24). First, by means of Eq. (27), the inverse of C can be approximated, up to second order in ϵ, as

$$\mathsf{C}^{-1} = \mathsf{I} - (\mathsf{A}_0 + \zeta \mathsf{A}_\zeta) + o(\epsilon^2). \tag{32}$$

Secondly, we can write the expression for the admissible virtual displacements as

$$\delta \boldsymbol{u} = \delta W \boldsymbol{E}_3 + (\delta U_\alpha + \zeta \delta U_{\zeta\alpha}) \boldsymbol{E}_\alpha + \zeta \delta W_\zeta \boldsymbol{E}_3 + o(L\epsilon^3), \tag{33}$$

for some arbitrary scalar functions δW, δU_α, $\delta U_{\zeta\alpha}$ and δW_ζ.

3.3 Scaling of the stress tensor components

To approximate the stress in the shallow regime, we first expand the Lagrange multiplier p around the initial pressure p_τ, which according to Eq.(16) equals r. Moreover, for physical consistency with the displacement field, we set an expansion for p that is affine with respect to ζ, consistently with Eq.(23). Hence, we write

$$p(\Theta^\alpha, \zeta) = r(\Theta^\alpha, \zeta) + p_0(\Theta^\alpha) + \zeta p_\zeta(\Theta^\alpha) + o(\mu\epsilon^2), \tag{34}$$

with $p_0 = O(\mu\epsilon^2)$ and $p_\zeta = O(\mu\epsilon)$. Then, using Eq.(17), (32) and (34), the second Piola-Kirchhoff stress tensor can be approximated as

$$\mathsf{S} := r\mathsf{I} - pJ\mathsf{C}^{-1} + \tau = r(\mathsf{A}_0 - Jp_0\mathsf{I}) + r\zeta(\mathsf{A}_\zeta - Jp_\zeta\mathsf{I}) + \tau + o(\mu\epsilon^2). \tag{35}$$

Notice that, since $J = O(1)$ (this can be deduced from Eq.(27)) the dominant part of the stresses induced by elastic deformations, namely $\hat{\mathsf{S}} = \mathsf{S} - \tau$, is of second order: $\hat{\mathsf{S}} = O(\epsilon^2\mu)$.

We are left with discussing the missing ingredient that is necessary for the dimensional reduction procedure, namely, the scaling for the initial stress tensor τ. Let us first write

τ in the contravariant base along the coordinate lines:

$$\tau = \tau_{ij} \bar{\boldsymbol{G}}^i \otimes \bar{\boldsymbol{G}}^j, \quad \tau_{ij} = \tau_{ij}(\Theta^\alpha, \zeta), \tag{36}$$

where τ_{ij} are the corresponding components. We assume that the tangent components of the initial stress are of the same order as the elastic stress induced by the planar displacement $\hat{\mathsf{S}}$, that is we set $\tau_{\alpha\beta} = O(\epsilon^2 \mu)$. This choice is motivated by the aim to investigate the stability of the reference configuration under the *residual* stress. In addition, if the τ's are residual, the leading order equilibrium equation (11) reads $\tau_{ij,i} = 0$, with $\tau_{i3}(\Theta^\alpha, \pm H) = 0$, and so it seems natural to take $\tau_{3\alpha} = O(\epsilon^3 \mu)$ and $\tau_{33} = O(\epsilon^4 \mu)$. As a first consequence of these choices, notice that the dominant contribution of the whole stress tensor S is of second order in ϵ, as can be seen from Eq.(35). Moreover, at the leading and next to leading orders, the equilibrium equation (11) can be expressed as a function of the average tangent stress components $T_{ij}(\Theta_\alpha) = \int_{-H}^{H} \tau_{ij} \, \mathrm{d}\zeta$ as:

$$T_{\alpha\beta,\alpha} = 0 \quad \text{at } O(\epsilon^2 \mu), \qquad T_{\alpha 3,\alpha} = 0 \quad \text{at } O(\epsilon^3 \mu). \tag{37}$$

Moreover, the invariants of the residual stress tensor have the following scaling:

$$I_{\boldsymbol{\tau}1} = \tau_{\alpha\alpha} = O(\mu\epsilon^2), \quad I_{\boldsymbol{\tau}2} = o(\mu\epsilon^2), \quad I_{\boldsymbol{\tau}3} = o(\mu\epsilon^2), \tag{38}$$

so that, the leading order expression of r in (15) is given by :

$$r = \mu - \frac{\tau_{\alpha\alpha}}{3} + o(\mu\epsilon^2). \tag{39}$$

In the following, we use these scaling assumptions to derive a rigorous asymptotic expansion of the three-dimensional boundary value problem given by (18).

3.4 Variational derivation of the nonlinear shallow shell equations

First, let us rewrite the balance equations in (18) according to the variational framework. To this purpose, let us introduce the *total* free energy

$$E = \int_{\omega_\tau} \int_{-H}^{H} (\psi(\mathsf{F}, \tau) - p(J-1))\, \mathrm{d}\zeta\, \mathrm{d}\bar{A} - \int_{\omega^\pm} \boldsymbol{\ell} \cdot \boldsymbol{u}\, \mathrm{d}\bar{a} - \int_{-H}^{H} (\int_{\partial\omega} \boldsymbol{h} \cdot \boldsymbol{u}\, \mathrm{d}|\partial\omega|)\, \mathrm{d}\zeta, \quad (40)$$

where the tractions $\boldsymbol{l}$ have been split into $\boldsymbol{\ell}$ and $\boldsymbol{h}$: $\boldsymbol{\ell} = \ell_\alpha \boldsymbol{E}_\alpha + \ell_3 \boldsymbol{E}_3$ denote the tractions on the surfaces $\omega^\pm := \omega \times \{\pm H\}$, and $\boldsymbol{h} = h_\alpha \boldsymbol{E}_\alpha + h_3 \boldsymbol{E}_3$ the tractions on $\partial\omega \times [-H, H]$. Moreover $\mathrm{d}\bar{A}$ and $\mathrm{d}\bar{a}$ are the reference and current area elements defined as $\mathrm{d}\bar{A} = \bar{G}\, \mathrm{d}\Theta$ and $\mathrm{d}\bar{a} = \bar{g}\, \mathrm{d}\Theta$, respectively.

Let us now rewrite the three-dimensional elastic boundary value problem stated in Eq.(18) as the stationarity of total free energy with respect to any admissible variation of the deformation and the pressure p. It reads:

$$\int_{\omega_\tau} \int_{-H}^{H} \frac{1}{2} \operatorname{tr}(\mathsf{S}\, \delta\mathsf{C})\, \mathrm{d}\zeta\, \mathrm{d}\bar{A} - \mathcal{L}[\delta\boldsymbol{u}] = 0 \qquad \forall \delta\boldsymbol{u}, \quad (41)$$

$$\int_{\omega_\tau} \int_{-H}^{H} \delta p (J-1)\, \mathrm{d}\zeta\, \mathrm{d}\bar{A} = 0 \qquad \forall \delta p \quad (42)$$

where

$$\mathcal{L}[\delta\boldsymbol{u}] := \int_{\omega^\pm} \boldsymbol{\ell} \cdot \delta\boldsymbol{u}\, \mathrm{d}\bar{a} + \int_{-H}^{H} (\int_{\partial\omega} \boldsymbol{h} \cdot \delta\boldsymbol{u}\, \mathrm{d}|\partial\omega|)\, \mathrm{d}\zeta,$$

$\delta\mathsf{C}$ being the variation of the conjugate strain measure, namely, the right Cauchy-Green tensor, and $\delta\boldsymbol{u}$ the variation of the displacement $\boldsymbol{u} := \boldsymbol{x} - \boldsymbol{X}$.

It is clear by looking at equations (27), (35) and (41) that the leading order contribution of the power expended by internal stresses is $O(\mu\epsilon^5)$. Indeed, we already mentioned in Section 3.3, that S is of second order in ϵ as well as the admissible variation of the Cauchy strain, as evident from Eq.(27). Consequently the magnitude of the traction loads

$\boldsymbol{\ell}$ and $\boldsymbol{h}$ must be chosen accordingly, so that the load power $\mathcal{L}$ balances out the internal power. Specifically we must choose $\ell_3 = O(\mu L\epsilon^4)$, $\ell_\alpha, h_3 = O(\mu L\epsilon^3)$ and $h_\alpha = O(\mu L\epsilon^2)$. This fact can be easily verified by checking that the leading order term of the load power $\mathcal{L}$ is infact $O(\mu\epsilon^5)$. Indeed, once we recognize that $\mathrm{d}\bar{A} = \mathrm{d}\Theta + O(H^2)$, $\mathrm{d}\bar{a} = \mathrm{d}\Theta + O(H^2)$, $\mathrm{d}|\partial\omega| = \mathrm{d}|\partial\mathcal{P}| + O(\epsilon H)$ and by means of formula (33), we can write the leading order term of $\mathcal{L}$ as

$$\begin{aligned}\mathcal{L} = &\int_{\mathcal{P}} \left(\tilde{\ell}_3 \delta W + \tilde{\ell}_\alpha \delta U_\alpha - H \underset{\sim}{\ell}_\alpha \delta W_{,\alpha}\right) \mathrm{d}\Theta + \\ &+ \int_{\partial\mathcal{P}} \left(\mathfrak{h}_3 \delta W + \mathfrak{h}_\alpha \delta U_\alpha - \mathfrak{m}_\alpha \delta W_{,\alpha}\right) \mathrm{d}|\partial\mathcal{P}|,\end{aligned} \tag{43}$$

where we defined the operators $\tilde{f} := f^+ + f^-$ and $\underset{\sim}{f} := (f^+ - f^-)$ [1] , and the boundary tractions and torques

$$\mathfrak{h}_i = \int_{-H}^{H} h_i \,\mathrm{d}\zeta, \qquad \mathfrak{m}_\alpha = \int_{-H}^{H} h_\alpha \zeta \,\mathrm{d}\zeta, \tag{44}$$

respectively. Eventually, the aforementioned choice for the scalings of the loads becomes apparent once we look at the leading order of $\mathcal{L}$ as written in Eq.(43). Given our assumptions, the load power of order $O(\mu\epsilon^5)$.

3.4.1 Boundary conditions and incompressibility constraint

Here we exploit the boundary conditions and the incompressibility constraint to derive an expression for the Cauchy-Green strain and the Piola-Kirchoff stress solely in terms of U_α and W.

The boundary conditions can be expressed by equating the work performed by the tractions $\mathcal{L}$ to the one performed by the stresses on the boundary. In particular, they must be of the same order in ϵ, that is $O(\mu\epsilon^5)$. Let us focus on the normal boundary, i.e.

[1] For each generic field ϕ we denote with ϕ^+ (ϕ^-) the quantity $\phi|_{\zeta=1}$ ($\phi|_{\zeta=-1}$)

$\omega^+ \cup \omega^-$, where $\boldsymbol{N} = \boldsymbol{G}_3$. The power of the stresses on the boundary must then satisfy

$$\int_{\omega^\pm} \boldsymbol{N}\mathsf{P} \cdot \delta\boldsymbol{u}\, \mathrm{d}\bar{a} = O(\mu\epsilon^5). \tag{45}$$

A straightforward computation shows that the above formula forces the *lower order terms* of $\boldsymbol{N}\,\mathsf{P}$ to vanish on the boundary. Specifically, we need $(\boldsymbol{N}\,\mathsf{P}) \cdot \bar{\boldsymbol{G}}_\alpha$ to vanish up to first order in ϵ, thus leading to:

$$U_{\zeta\alpha} = -W_{,\alpha}. \tag{46}$$

In passing, notice that the above formula expresses the classical Kirchhoff-Love hypothesis, that is here justified by vanishing of the leading order shear stress components on the boundary. On the other hand, (45) forces $(\boldsymbol{N}\,\mathsf{P}) \cdot \boldsymbol{N}$ to vanish up to second order in ϵ, which leads to

$$p_0 = -\mu U_{\alpha,\alpha} + \mu W_\zeta \quad \text{and} \quad p_\zeta = \mu W_{\alpha,\alpha}. \tag{47}$$

Finally, we have to impose the incompressibility constraint expressed in Eq.(42). First, by using (27), we expand the Jacobian as $J = 1 + \operatorname{tr}\mathsf{A}_0 + \zeta \operatorname{tr}\mathsf{A}_\zeta + O(\epsilon^4)$. Next, we take as admissible pressure variations all the functions δp such that $\delta p(\Theta, \zeta) = \delta p_0(\Theta) \sim O(\mu\epsilon^2)$. Finally, we integrate equation (42) along ζ and approximate it up to order $O(\epsilon^5)$ thus obtaining $\operatorname{tr}\mathsf{A}_0 = 0$. If we make explicit the trace of A_0 and equate it to zero we get

$$W_\zeta = U_{\alpha,\alpha} - g_{\alpha\alpha} + G_{\alpha\alpha}. \tag{48}$$

At this point, equations (46),(47) and (48) give us all the ingredients to express the kinematics just in term of U_α and W, as previously anticipated. In particular, neglecting terms of order $o(\epsilon^2)$, the metric components of the middle surface in the reference and spatial configurations read:

$$G_{\alpha\beta} = \delta_{\alpha\beta} + Z_{,\alpha}Z_{,\beta}, \qquad g_{\alpha\beta} = \delta_{\alpha\beta} + U_{\alpha,\beta} + U_{\beta,\alpha} + (W+Z)_{,\alpha}(W+Z)_{,\beta}, \tag{49}$$

respectively. Consequently, the right Cauchy-Green strain tensor is given by $\mathsf{C} = \mathsf{I} + \mathsf{A}_0 + \zeta \mathsf{A}_\zeta + o(\epsilon^2)$, where:

$$\mathsf{A}_0 = (g_{\alpha\beta} - G_{\alpha\beta})\boldsymbol{E}_\alpha \otimes \boldsymbol{E}_\beta - (g_{\alpha\alpha} - G_{\alpha\alpha})\boldsymbol{E}_3 \otimes \boldsymbol{E}_3, \tag{50}$$

$$\mathsf{A}_\zeta = -2W_{,\alpha\beta}\boldsymbol{E}_\alpha \otimes \boldsymbol{E}_\beta. \tag{51}$$

In turn, also the expressions for admissible displacements and strain can be updated and expressed as a function of the variations $(\delta U_\alpha, \delta W)$ of the planar and normal components of the displacement. We get:

$$\delta \boldsymbol{u} = \epsilon \delta W \boldsymbol{E}_3 + \epsilon^2(\delta U_\alpha - \zeta \delta W_{,\alpha})\boldsymbol{E}_\alpha + o(\epsilon^2 L), \tag{52}$$

$$\delta \mathsf{C} = (\delta U_{\alpha,\beta} + \delta U_{\beta,\alpha} + \delta W_{,\alpha}(Z+W)_{,\beta} + \delta W_{,\beta}(Z+W)_{,\alpha} - 2\zeta \delta W_{,\alpha\beta})\, \boldsymbol{E}_\alpha \otimes \boldsymbol{E}_\beta + o(\epsilon^2). \tag{53}$$

Lastly, once the the kinematics in known it is immediate to derive and expression for S in terms of U_α and W. First, the pressure terms in Eq.(47), p_0 and p_ζ, can be rephrased as

$$p_0 = \mu(G_{\alpha\alpha} - g_{\alpha\alpha}), \qquad p_\zeta = \mu\, W_{,\alpha\alpha}. \tag{54}$$

Eventually,

$$\mathsf{S} = \mathsf{S}_0 + \zeta\, \mathsf{S}_\zeta + \tau^{(2)} + o(\mu\epsilon^2), \tag{55}$$

with:

$$\mathsf{S}_0 = \mu\left((g_{\gamma\gamma} - G_{\gamma\gamma})\delta_{\alpha\beta} + \mu(g_{\alpha\beta} - G_{\alpha\beta})\right) \boldsymbol{E}_\alpha \otimes \boldsymbol{E}_\beta, \tag{56}$$

$$\mathsf{S}_\zeta = -2\mu W_{,\alpha\beta}\boldsymbol{E}_\alpha \otimes \boldsymbol{E}_\beta, \tag{57}$$

$$\boldsymbol{\tau}^{(2)} = \tau_{\alpha,\beta}\boldsymbol{E}_\alpha \otimes \boldsymbol{E}_\beta. \tag{58}$$

We can rewrite the leading order contribution $O(\mu\epsilon^5)$ of the potential energy variation, as the sum of two contributions arising from the tangent (δU_α) and normal (δW)

variations, respectively. In the following we consider these two variation separately, for the sake of simplicity.

3.4.2 Stretching equation

The tangent contribution in (41) is the virtual work made by the planar stresses onto planar variations δU_α. The planar equilibrium is then expressed by

$$\int_{\mathcal{P}} (N_{\alpha\beta} + T_{\alpha\beta})(\delta U_{\alpha,\beta} + \delta U_{\beta,\alpha})\, \mathrm{d}\Theta - \int_{\mathcal{P}} \tilde{\ell}_\beta \delta U_\beta \, \mathrm{d}\Theta - \int_{\partial\mathcal{P}} \mathfrak{h}_\alpha \, \mathrm{d}|\partial\mathcal{P}| = 0, \qquad \forall \delta U_\alpha, \quad (59)$$

with:

$$N_{\alpha\beta} = \int_{-H}^{H} S_{0\alpha\beta}\, \mathrm{d}\zeta = 2HS_{0\alpha\beta}.$$

Integrating by parts Eq.(59) and taking into account Eq.(37), we get the in-plane equilibrium

$$N_{\alpha\beta,\alpha} + \tilde{\ell}_\beta = 0 \qquad \text{in } \mathcal{P}, \quad (60)$$

$$(N_{\alpha\beta} + T_{\alpha\beta}) n_\beta = \mathfrak{h}_\alpha \qquad \text{in } \partial\mathcal{P}, \quad (61)$$

where $\boldsymbol{n}$ denotes the unit outer normal to $\partial\mathcal{P}$.

In the case of conservative external loads, instead of considering the above equation, we can rely on the existence of an Airy stress function defined as follows. First let us introduce the potential functions L^+ and L^- for the external loads so that

$$\boldsymbol{\ell}^{\pm} = \nabla L^{\pm}. \quad (62)$$

Then we build an Airy function so as to satisfy

$$\chi_{,22} = \Sigma_{11}, \quad \chi_{,11} = \Sigma_{22}, \quad -\chi_{,12} = \Sigma_{12} = \Sigma_{21}, \quad (63)$$

where $\Sigma_{\alpha\beta} := N_{\alpha\beta} + T_{\alpha\beta} + \tilde{L}\delta_{\alpha\beta}$. Thanks to the Airy potential the stress defined above automatically satisfies Eq.(60). However, some compatibility conditions for χ must be added, namely, $\nabla_t^4\chi = \Sigma_{11,22} + \Sigma_{22,11} - 2\Sigma_{12,12}$, where ∇_t is the gradient operator in $\mathbb{R}^2$.[2] Using Eq.(60,63), we finally get the following expression for the compatibility condition:

$$\boxed{-\nabla_t^4\chi = 12H\mu\,[W, Z + W/2] - \mu C_G - \frac{1}{2}\tilde{L}_{,\alpha\alpha}} \tag{64}$$

In the above formula, $[\cdot,\cdot]$ denotes the already mentioned bilinear operator, namely, $[a,b] = \frac{1}{2}(a_{,11}b_{,22} + a_{,22}b_{,11} - 2a_{,12}b_{,12})$ while $C_G := (T_{11,22} + T_{22,11} - 2T_{12,12})/\mu$ and plays the role of a spontaneous Gaussian curvature imposed by the tangent residual stress.

3.4.3 Bending equation

As for the stretching counterpart, the transverse contribution in (41) is the virtual work made by the transverse stresses onto transverse variations δW. It reads

$$\begin{aligned}&\int_{\mathcal{P}} \left[(N_{\alpha\beta} + T_{\alpha\beta})(Z+W)_{,\beta}\,\delta W_{,\alpha} + \left(\frac{4}{3}\mu H^3 W_{,\alpha\beta} - M_{\alpha\beta}\right)\delta W_{,\alpha\beta}\right] \mathrm{d}\Theta \\ &- \int_{\mathcal{P}} \left(\tilde{h}_3\delta W - H\underset{\sim}{h}_\alpha \delta W_{,\alpha}\right) \mathrm{d}\Theta - \int_{\partial\mathcal{P}} (\mathfrak{h}_3\delta W - \mathfrak{m}_\alpha\delta W_{,\alpha})\,\mathrm{d}|\partial\mathcal{P}| = 0 \qquad \forall\delta W,\end{aligned} \tag{65}$$

where we denoted by $\mathsf{M} = M_{\alpha\beta}\boldsymbol{E}_\alpha\otimes\boldsymbol{E}_\beta$ the tangent torque tensor imposed by the residual stress, whose cartesian components are defined as

$$M_{\alpha\beta} = \int_{-H}^{H} \tau_{\alpha\beta}\zeta\,\mathrm{d}\zeta. \tag{66}$$

[2]Notice that, since $\Sigma_{\alpha\beta}$ is divergence free, we have that μC_G can be conveniently rewritten as $\Sigma_{11,22} + \Sigma_{22,11} - 3\Sigma_{12,12} - 1/2(\Sigma_{11,11} + \Sigma_{22,22})$.

Integration by parts of Eq.(65) eventually leads to the strong form of the equations for transverse equilibrium of the shell. They read

$$\frac{4}{3}H^3\mu\nabla_t^4 W - M_{\alpha\beta,\alpha\beta} - \left[(N_{\alpha\beta}+T_{\alpha\beta})(Z+W)_{,\beta}\right]_{,\alpha} - \tilde{\ell}_3 - H\underset{\sim}{\ell}_{\alpha,\alpha} = 0 \qquad \text{in } \mathcal{P}, \tag{67}$$

$$(N_{\alpha\beta}+T_{\alpha\beta})(Z+W)_{,\beta}\, n_\alpha - (\partial_\alpha m_{\alpha\beta})n_\beta - \partial_{\boldsymbol{t}}((m_{\alpha\beta}-\mathfrak{m}_\beta)n_\alpha t_\beta) = 0 \qquad \text{in } \partial\mathcal{P}, \tag{68}$$

$$(m_{\alpha\beta}n_\alpha - \mathfrak{m}_\beta)n_\beta = 0 \qquad \text{in } \partial\mathcal{P}. \tag{69}$$

where $\boldsymbol{t}$ is the tangent unit vector to $\partial\mathcal{P}$ and $m_{\alpha\beta} := 4/3\mu H^3 W_{,\alpha\beta} - M_{\alpha\beta}$. Finally, exploiting the definition of the Airy stress function χ and of the load potential L we get the following formulation for transverse equilibrium in Eq.(67)

$$\boxed{\frac{4}{3}H^3\mu\nabla_t^4 W - \nabla_t\cdot\nabla_t\cdot\mathbf{M} - 2[\chi, Z+W] + \left(\tilde{L}_{,\alpha}(Z+W)_{,\alpha}\right)_{,\alpha} - \tilde{L}_{,3} - H\underset{\sim}{L}_{,\alpha\alpha} = 0} \tag{70}$$

We finally remark that we can define a quantity C_M by setting $\frac{8}{3}\mu\nabla_t^2 C_M := \nabla_t\cdot\nabla_t\cdot\mathbf{M}$ which represents the spontaneous mean curvature driven by the torque imposed by the residual stress.

4 Physical examples

The dimensionally reduced shell model consists of two *coupled*, nonlinear, partial differential equations, Eq.(64) and Eq.(70), in the unknowns χ and W, to be solved together with the boundary conditions given by Eqs.(68) and (69). The governing equations Eq.(64) and Eq.(70) highlight the interplay between initial stresses and the nonlinear deformation of shallow shells. In Eq.(64), the compatibility condition explicitly includes the contribution of the tangent residual stress components through the spontaneous Gaussian curvature C_G, defined as a function of the residual stress tensor. This term imposes a geometric constraint that is absent in the classical MvK equations. Similarly, Eq. (70)

introduces the effect of residual stress through the torque tensor, which contributes to the spontaneous mean curvature C_M. These contributions encapsulate the role of the initial stress in shaping the shell's morphology, altering the equilibrium configuration and stability characteristics compared to the stress-free case. In the absence of initial stresses, the terms C_G and C_M reduce to zero, and we recover the classical MvK equations for shallow shells, which describe deformations driven solely by external loads and intrinsic material properties. This demonstrates the consistency of our framework with established shell theories, while also extending their applicability to contexts involving initial stresses. The following physical examples are designed to illustrate different aspects of how initial stresses influence the deformation and the morphological transitions in shallow shells. Specifically, these examples address scenarios where initial stresses induce spontaneous curvature, affect buckling thresholds, and drive complex stability behaviors. By focusing on a twisted saddle-shaped shell and a pre-stressed cylindrical shell, we aim to provide a detailed exploration of the impact of initial stresses on both local and global mechanical responses, emphasizing their role in shaping the morphology and stability of shallow shells under various loading conditions.

4.1 Twisting and stretching of a saddle strip

Let us consider a shallow hyperbolic paraboloidal strip whose undeformed configuration has the following parametric expression:

$$Z(\Theta_1, \Theta_2) = \beta \Theta_1 \Theta_2,$$

with $|\Theta_1| \leq l_1$ and $|\Theta_2| \leq l_2$ (see Fig.2). For consistency to the shallowness assumption, we assume that $\beta \cdot \max[l_1, l_2] \sim \epsilon$. Moreover, the undeformed shallow shell is initially stressed with vanishing tangent torque tensor and the following average tangent stress

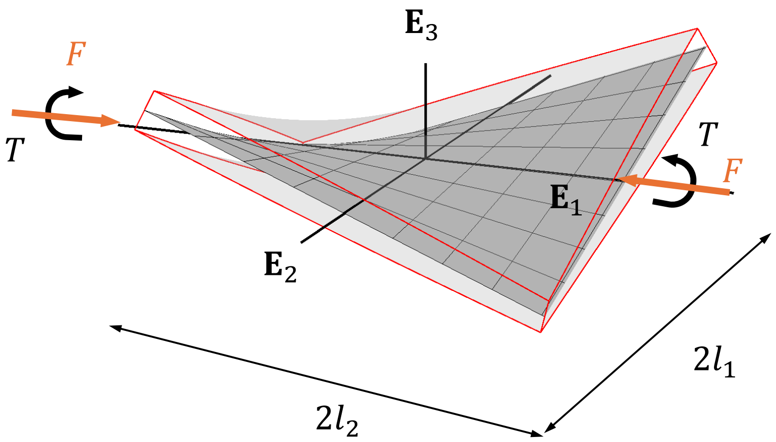

Figure 2: Sketch of the pre-twisted strip along with the Cartesian reference system and the resultant load F and torque T

components:

$$T_{11} = \mu c^2(\Theta_1^2 - l_1^2), \qquad T_{22} = \mu c^2(\Theta_2^2 - l_2^2), \qquad T_{12} = -\mu c^2 \Theta_1 \Theta_2, \tag{71}$$

with $c \sim \epsilon^{3/2}$. We remark that such an initial stress distribution admits an initial Airy stress function $\chi_i = \mu c^2(\Theta_1^2 - l_1^2)(\Theta_2^2 - l_2^2)/2$, inducing a positive spontaneous Gaussian curvature $C_G = 4c^2$.

We now seek for a solution assuming that the shell is free of edge tractions along $\Theta_2 = \pm l_2$ and it is subjected to self balancing resultant axial force F and torque T along $\Theta_1 = \pm l_1$. Hence, we make the following ansatz

$$W = \gamma \Theta_1 \Theta_2, \qquad \chi = \chi(\Theta_2). \tag{72}$$

Accordingly, equation (70) is trivially fulfilled, while the in-plane equilibrium (64) reads

$$\chi'''' = C, \qquad C := 12H\mu\gamma(\beta + \gamma/2) + 4\mu c^2. \tag{73}$$

Hence, upon integration of the Airy potential we get

$$\Sigma_{11} = \chi'' = A(\Theta_1) + B(\Theta_1)\Theta_2 + C\frac{\Theta_2^2}{2}, \qquad \Sigma_{22} = \Sigma_{12} = 0. \tag{74}$$

Finally, in order to express the global boundary conditions for the resultants F and T, we simply consider the natural boundary conditions in the equations (68),(69) and test them on infinitesimal isometries, namely, $\delta U_1(\Theta_1, \Theta_2) = \eta_1 + \Omega\Theta_2$, $\delta U_2(\Theta_1, \Theta_2) = \eta_2 - \Omega\Theta_1$ and $\delta W(\Theta_1, \Theta_2) = \eta_3 + \psi_1\Theta_1 + \psi_2\Theta_2$. In particular, considering rigid body rotations along the vertical axis $\boldsymbol{E}_3$ we get

$$\int_{-l_2}^{l_2} (\Theta_1\Sigma_{12} - \Theta_2\Sigma_{11})\, \mathrm{d}\Theta_2 = 0, \tag{75}$$

which leads to $B = 0$. Moreover, the balance of the traction forces F and the torque T can be expressed as

$$\int_{-l_2}^{l_2} \Sigma_{11}\, \mathrm{d}\Theta_2 = F \qquad \text{for } \Theta_1 = \pm l_1, \tag{76}$$

$$\int_{-l_2}^{l_2} \left((\Sigma_{1\beta}(Z + W)_{,\beta} - (\partial_\alpha m_{\alpha 2}))\, \Theta_2 + m_{1,2} \right) \mathrm{d}\Theta_2 = T \qquad \text{for } \Theta_1 = \pm l_1, \tag{77}$$

which rewrite as

$$2Al_2 + \frac{1}{3} l_2^3 \left(-4\mu c^2 + 12H \left(\beta + \frac{\gamma}{2} \right) \gamma\mu \right) = F, \tag{78}$$

$$\frac{2}{15} \left(5Al_2^3(\beta + \gamma) + 20 l_2 H^2 \gamma\mu + 3l_2^5(\beta + \gamma)(-2\mu c^2 + 3H\gamma\mu(2\beta + \gamma)) \right) = T. \tag{79}$$

The above equation can be solved in the unknowns γ and A once F and T are given.

In particular, we can easily find the solution in the case of vanishing traction force, i.e. by setting $F = 0$ in Eq.(78), and hence recover an expression for T as a function of γ

from Eq.(79). In this case, we obtain the following expressions

$$A = -\frac{1}{3} l_2^2 \left(2\mu c^2 + 6H\beta\gamma\mu + 3H\gamma^2\mu \right), \tag{80}$$

$$T = \frac{8}{45} l_2 \mu \left(15H^2\gamma + l_2^4(\beta+\gamma)(2c^2 + 3H\gamma(2\beta+\gamma)) \right). \tag{81}$$

Notice that, the above expressions are still meaningful in the undeformed case, i.e. for $\gamma = 0$, provided we apply the initial torque T_i given by

$$T_i = \frac{16}{45} \mu\beta c^2 l_2^5. \tag{82}$$

This means that the initial stress tensor given by the Airy stress function $\chi_i(\Theta_1, \Theta_2)$ can be transformed into a uniaxial stress tensor, given by $\chi_i(\Theta_2)$, by application of a torque T_i at the edges $\Theta_1 = \pm l_1$. The magnitude of such a required torque depends on the product between the initial and the spontaneous Gaussian curvatures.

4.2 Buckling of a pre-stressed shallow cylindrical sector

Let us consider a shallow cylindrical sector, whose parametrization at the leading order in ϵ can be expressed as:

$$Z(\Theta_1, \Theta_2) = R_0 - \Theta_1^2/(2R_0),$$

with $(\Theta_1, \Theta_2) \in [-l_1, l_1] \times [-l_2, l_2]$, and $R_0 \sim \max[l_1, l_2]/\epsilon$ (see Fig.3). The shell is subjected to initial stresses arising from the presence of a compressive axial load β and

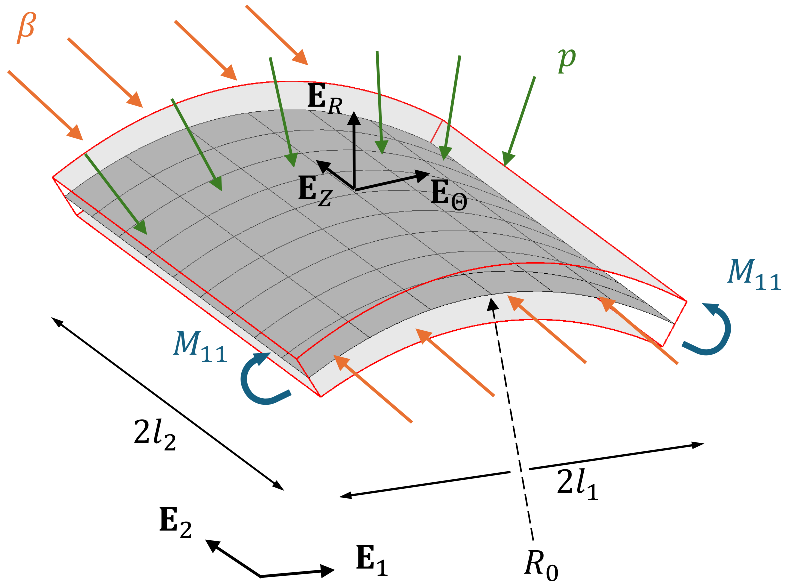

Figure 3: Sketch of the cylindrical shell along with its Cartesian dimensions l_1 e l_2 and the cylindrical reference system $(\boldsymbol{E}_R, \boldsymbol{E}_\Theta, \boldsymbol{E}_Z)$. We also illustrate the distributed axial load β, the normal pressure p, and the residual torque M_{11}.

an inward outer pressure p. The three-dimensional initial stress state is given by

$$\tau_{RR} = \frac{\alpha\mu}{R_0^2}(R - R_i)(R_e - R - \frac{pR_0^2}{2H\alpha\mu}), \tag{83}$$

$$\tau_{\Theta\Theta} = -\frac{p(R_i - 2R)}{2H} - \frac{\alpha\mu}{R_0^2}(R_iR_e - 2(R_i + R_e)R + 3R^2), \tag{84}$$

$$\tau_{ZZ} = -\beta, \tag{85}$$

where $R_i = (R_0 - H)$ and $R_e = (R_0 + H)$ are the internal and external radii, respectively. The former expressions are derived assuming that the initial stress tensor in the undeformed configuration is divergence free. In the shallow shell limit when $\epsilon = H/l_1 \ll 1$, the above stress distribution implies that:

$$\tau_{33} = O(\mu\epsilon^4), \qquad \tau_{11} = -\frac{pR_0}{2H} - 2\frac{\alpha\mu}{R_0}\zeta + o(\mu\epsilon^2), \qquad \tau_{22} = -\beta + o(\mu\epsilon^2), \tag{86}$$

with $\alpha \sim 1$, $p \sim \epsilon^4$, $\beta \sim \epsilon^2$. Consequently, the shell is subjected to the following average in plane stresses and momenta

$$T_{11} = -pR_0, \qquad T_{22} = -2H\beta, \quad M_{11} = -\frac{4}{3}\mu H^3 \frac{\alpha}{R_0}. \tag{87}$$

Accordingly, the shallow shell equations (64,70) read

$$-\nabla^4\chi = 12\mu H \left(\frac{W_{,11}W_{,22}}{4} + \frac{1}{2}W_{,22}\left(\frac{W_{,11}}{2} - \frac{1}{R_0}\right) - \frac{W_{,12}^2}{2} \right), \tag{88}$$

$$\frac{4}{3}H^3\mu\nabla^4 W - \left(\chi_{,11}W_{,22} + \chi_{,22}\left(W_{,11} - \frac{1}{R_0}\right) - 2\chi_{,12}W_{,12} \right) + p = 0. \tag{89}$$

In the following, we provide a linear bifurcation analysis to identify the critical loads for the buckling of the shell in three illustrative cases, for $p = 0$, $\beta = 0$ and $\beta, p \neq 0$.

4.2.1 Longitudinal buckling for p=0

Let us consider the regime where p is vanishing and hence, only the axial compressive load β and the residual torque M_{11} are present. Consequently, the Airy function of the initial stresses χ_i is given by $\chi_i = -H\beta\Theta_1^2$.

Let us search for a base solution (χ_0, W_0) with $\mathfrak{m}_\alpha = 0$ at the boundary $\Theta_1 = \pm l_1$, i.e. $m_{\alpha\beta} = -4/3\mu H^3 W_{0,\alpha\beta} + M_{\alpha\beta} = 0$. Hence, the base solution must satisfy

$$4/3\mu H^3 W_{0,11}(\pm l_1, \Theta_2) = M_{11}, \qquad 4/3\mu H^3 W_{0,22}(\Theta_1, \pm l_2) = 0, \qquad W_0(0) = 0, \tag{90}$$

which are trivially solved by

$$W_0 = -\frac{\alpha}{R_0}\frac{\Theta_1^2}{2}, \qquad \chi_0 = -H\beta\Theta_1^2. \tag{91}$$

Then, we linearize the equations Eqs.(88), (89) around this base solution by superposing a small perturbation in the following form:

$$W(\Theta_1, \Theta_2) = W_0(\Theta_1) + \delta W(\Theta_2), \qquad \chi(\Theta_1, \Theta_2) = \chi_0(\Theta_1) + \delta\chi(\Theta_2). \tag{92}$$

The resulting incremental equations at the leading order read:

$$\delta\chi'''' - \frac{6\mu H}{R_\alpha}\delta W'' = 0, \qquad \frac{4}{3}\mu H^3 \delta W'''' + \frac{\delta\chi''}{R_\alpha} + 2H\beta\delta W'' = 0, \tag{93}$$

where the primes denote differentiation with respect to Θ_2, and R_α is defined as

$$R_\alpha = \frac{R_0}{1+\alpha}. \tag{94}$$

The equations (93) are complemented with the following incremental boundary conditions stemming from (90)

$$\delta W(0) = \delta W(l_2) = 0 \qquad \text{and} \qquad \delta W''(0) = \delta W''(l_2) = 0. \tag{95}$$

The linear bifurcation analysis in then conducted by searching for solutions of the form $\delta W(\Theta_2) = A\sin(k\Theta_2)$ and $\delta\chi(\Theta_2) = B\sin(k\Theta_2)$ from which the following expression for the critical loads is deduced

$$\beta_n = \frac{9\mu + 2H^2 k_n^4 R_\alpha^2 \mu}{3k_n^2 R_\alpha^2}, \qquad k_n = \frac{n\pi}{l_2}. \tag{96}$$

As for the minimum critical load we get

$$\beta_{cr} = \frac{2\sqrt{2}H\mu}{R_\alpha}, \qquad k_{cr} = \sqrt{\frac{3}{\sqrt{2}HR_\alpha}}, \tag{97}$$

whose scaling with H is consistent with the classical results in mechanical literature in the absence of residual stress, see for instance [23, 40].

4.2.2 Circumferential buckling for β=0

Let us now consider the regime where $\beta = 0$ while both the circumferential compressive load p and the residual torque M_{11} are present. Consequently, the Airy stress function of the initial stresses χ_i is given by $\chi_i = -pR_0\Theta_2^2/2$.

As in the previous example we consider a base solution (χ_0, W_0) satisfying $\mathfrak{m}_\alpha = 0$ at the boundary, that is

$$W_0 = -\frac{\alpha}{R_0}\frac{\Theta_1^2}{2}, \qquad \chi_0 = -pR_\alpha\Theta_2^2/2, \tag{98}$$

with R_α defined as above. Then, we linearize the equations Eqs.(88), (89) around this base solution by superposing a small perturbation in the following form:

$$W(\Theta_1, \Theta_2) = W_0(\Theta_1) + \delta W(\Theta_1), \qquad \chi(\Theta_1, \Theta_2) = \chi_0(\Theta_2) + \delta\chi(\Theta_1). \tag{99}$$

The resulting incremental equations at the leading order read:

$$\delta\chi'''' = 0, \qquad \frac{4}{3}\mu H^3\delta W'''' + pR_\alpha\delta W'' = 0, \tag{100}$$

where the primes denote differentiation with respect to Θ_1. The equations (100) are complemented with the following incremental boundary conditions

$$\delta W(-l_1) = \delta W(l_1) = 0 \qquad \text{and} \qquad \delta W''(-l_1) = \delta W''(l_1) = 0. \tag{101}$$

The linear bifurcation analysis in then conducted by searching for solutions of the form $\delta W(\Theta_1) = A\cos(k\Theta_1)$ and $\delta\chi(\Theta_1) = B\cos(k\Theta_1)$ from which the following expression for the critical loads is deduced

$$p_m = \frac{4H^3\mu k_m^2}{3R_\alpha}, \qquad k_m = \frac{\pi(2m+1)}{2l_1}. \tag{102}$$

As for the minimum critical load we get

$$p_{cr} = \frac{H^3\pi^2\mu}{3l_1^2 R_\alpha}, \qquad k_{cr} = \frac{\pi}{2l_1}. \tag{103}$$

4.2.3 Two-dimensional buckling for $\beta, p \neq 0$

Let us now consider the case when both $\beta, p \neq 0$. The initial Airy potential is given by $\chi_i = -pR_0\Theta_2^2/2 - H\beta\Theta_1^2$. As in the previous example we take a base solution such that $\mathfrak{m}_\alpha = 0$ at the boundary, that is given by

$$W_0 = -\frac{\alpha}{R_0}\frac{\Theta_1^2}{2}, \qquad \chi_0 = -pR_\alpha\frac{\Theta_2^2}{2} - H\beta\Theta_1^2. \tag{104}$$

Linearization around W_0 and χ_0 leads to the following incremental equations:

$$-\nabla^4\delta\chi = -\frac{6\mu H}{R_\alpha}\delta W_{,22}, \tag{105}$$

$$\frac{4}{3}\mu H^3\nabla^4\delta W + 2H\beta\delta W_{,22} + pR_\alpha\delta W_{,11} + \frac{\delta\chi_{,22}}{R_\alpha} = 0, \tag{106}$$

together with the incremental boundary conditions

$$\delta W(\pm l_1, \Theta_2) = \delta W_{,11}(\pm l_1, \Theta_2) = 0, \tag{107}$$

$$\delta W(\Theta_1, \gamma) = \delta W_{,22}(\Theta_1, \gamma) = 0, \quad \gamma = (0, l_2). \tag{108}$$

Finally, searching for solutions in the form

$$\delta W = E\cos(k_1\Theta_1)\sin(k_2\Theta_2), \qquad \delta\chi = F\cos(k_1\Theta_1)\sin(k_2\Theta_2), \tag{109}$$

leads to the following dispersion relation between α, β and p

$$\frac{18H\mu k_2^4}{(k_1^2+k_2^2)^2 R_\alpha}+R_\alpha(-3k_2^2 pR_\alpha-6Hk_1^2\beta+4H^3(k_1^2+k_2^2)^2\mu)=0, \tag{110}$$

with $k_1=\frac{n\pi}{l_1}$ and $k_2=\frac{(2m+1)\pi}{2l_2}$. Hence, we can compute the expressions for the critical loads as a function of the shape factors $r=l_2/l_1$ and $\rho=R_\alpha/l_1$. In particular we get

$$p^*_{nm}(\beta^*)=-\frac{4}{3\pi^2(1+2m)^2\rho^2}\left(\frac{6n^2\epsilon^2\pi^2\rho\beta^*}{r^2}-f\right), \tag{111}$$

$$\beta^*_{nm}(p^*)=-\frac{r^2}{6\epsilon n^2\pi^2\rho}\left(\frac{3(1+2m)^2p^*\pi^2\rho^2}{4}-f\right), \tag{112}$$

with:

$$f=\frac{288\epsilon n^4}{\rho((r+2rm^2)+4n^2)^2}+\frac{1}{4}\epsilon^3\pi^4\left((1+2m)^2+\frac{4n^2}{r^2}\right).$$

where $p^*=p/\mu$ and $\beta^*=\beta/\mu$. In Figure 4 we plot the critical loads in equations (111),(112) versus the corresponding one-dimensional counterparts in equations (97) and (103), which rewrite

$$\beta^{*(1D)}_{cr}=2\sqrt{2}\frac{\epsilon}{\rho}, \qquad p^{*(1D)}_{cr}=\frac{\pi^2}{3}\frac{\epsilon^3}{\rho}, \tag{113}$$

highlighting that the one-dimensional instability modes are indeed the critical ones.

5 Concluding remarks

In summary, we derived a nonlinear morphoelastic theory for an incompressible elastic shallow shells with initial stress in the reference configuration. We performed a geometric dimensional reduction by assuming that the small thickness ratio $\epsilon=H/L$ of the shell is of the same order as the slope of the reference middle surface. We later imposed a constitutive assumption for an initially stressed neo-Hookean material as developed in [35, 15] to perform a rigorous asymptotic expansion of the three-dimensional potential energy of the shell. We derived the leading order scaling for the rotation vectors and the

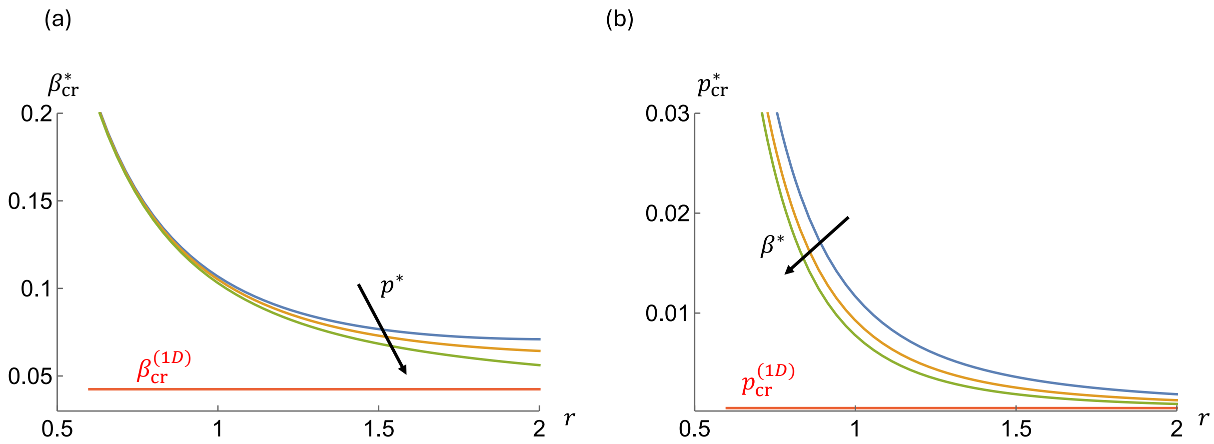

Figure 4: Plots of the critical traction loads β^*_{cr} (left) and p^*_{cr}(right) versus the aspect ratio r, computed at $\epsilon = 0.1$, $\rho = 6.66$. (a) The solid curves depict β^*_{cr} for $p^* = \{5 \times 10^{-5}, 2.5 \times 10^{-4}, p^{(1D)}_{cr}\}$, with $p^{(1D)}_{cr} = 4.93 \times 10^{-4}$. (b) The solid curves depict p^*_{cr} for $\beta^* = \{0.01, 0.03, \beta^{(1D)}_{cr}\}$, with $\beta^{(1D)}_{cr} = 0.0424$.

hydrostatic pressure from the incompressibility constraint and the boundary condition at the normal boundary of the shell. After application of the principle of stationary energy for admissible variation of the tangent and normal displacement fields with respect to the reference middle surface, we derived the generalised Marguerre-von Karman equilibrium equations (64) and (70) accounting for the effect of initial stresses. We highlight that the initial stress distribution can physically impose both a mean and a Gaussian curvature to the shell, which are generally not compatible with the existence of a stress free configuration.

The derived nonlinear equations were explicitly solved for two physical models: a twisted hyperbolic paraboloidal strip and a pre-stressed shallow cylindrical sector. In the twisted hyperbolic paraboloidal strip, the analysis demonstrates that the distribution of initial stresses can be effectively investigated through non-invasive torsion tests. The initial stress induces a spontaneous Gaussian curvature, which modifies the Airy stress function and leads to measurable changes in the deformed equilibrium shape. The nonlinear coupling between the applied torque and the initial stress distribution highlights how torsion-induced deformations encode information about the underlying stress state. For the pre-stressed shallow cylindrical sector, the initial stresses influence the critical buckling loads, altering both the longitudinal and circumferential instability modes. The analysis demonstrates that the coupling between initial stress, curvature, and deformation amplifies or mitigates instability depending on the stress distribution and shell geometry, providing a nuanced understanding of how morphologies evolve under combined mechanical and geometric effects.

These examples demonstrated how initial stress distributions drive the emergence of spontaneous curvatures, influencing the structural behavior of the shells. Unlike existing approaches that impose an incompatible growth metric [11, 22, 12], our method directly incorporates initial stresses into the governing equations, offering a direct link between the stress state and the resulting deformations. This framework avoids the need for prescribing a priori geometric incompatibilities and instead provides a physically consistent representation of systems where initial stresses naturally arise, such as in growth-induced morphological transitions. Furthermore, the proposed approach enables the determination of initial stress from non-invasive tests that measure deformation fields under controlled loading conditions. Its suitability for solving direct and inverse mechanical problems makes the proposed framework particularly suitable for applications where initial stresses play a critical role but cannot be directly measured.

In future works, we aim to explore the importance of the residual stresses in driving morphological transitions by solving the resulting nonlinear shallow shell equation in simple biological system models. Since the residual stresses can be controlled by external factors in many modern techniques of digital manufacturing, we believe that the proposed morphoelastic theory may also enable to achieve a robust adaptive control of the shell metric by external multiphysics stimuli.

Acknowledgements

This work was partly supported by MUR through the grants PRIN 2020 Research Project MATH4I4 and Dipartimento di Eccellenza 2023-2027. P. Ciarletta and D. Andrini are members of the group GNFM at INDAM. X. Chen acknowledges the support of National Natural Science Foundation of China (Grant No. 12272055), and Guangdong Provincial Key Laboratory of Interdisciplinary Research and Application for Data Science, BNU-HKBU United International College (Project No. 2022B1212010006).

References

[1] M. Amabili. *Nonlinear mechanics of shells and plates in composite, soft and biological materials*. Cambridge University press, Cambridge, 2018.

[2] D. Ambrosi, G. A. Ateshian, E. M. Arruda, S. C. Cowin, J. Dumais, A. Goriely, G. A. Holzapfel, J. D. Humphrey, R. Kemkemer, E. Kuhl, et al. Perspectives on biological growth and remodeling. *Journal of the Mechanics and Physics of Solids*, 59(4):863–883, 2011.

[3] M. Arroyo and A. DeSimone. Shape control of active surfaces inspired by the movement of euglenids. *Journal of the Mechanics and Physics of Solids*, 62:99–112, 2014.

[4] V. Balbi and P. Ciarletta. Morphoelasticity of intestinal villi. *Journal of the Royal Society Interface*, 12(106):20150287, 2015.

[5] K. Bathe. *Finite Element Procedures*. Klaus-Jurgen Bathe, 2014.

[6] P. Ciarlet. A justification of the von kármán equations. *Annales de la Faculté des Sciences de Toulouse*, 1:173–200, 1990.

[7] P. Ciarlet. *Mathematical Elasticity: Volume III: Theory of Shells*. Elsevier, 1997.

[8] P. Ciarlet and V. Lods. Asymptotic analysis of linearly elastic shells. i. justification of membrane shell equations. *Archive for Rational Mechanics and Analysis*, 73:349–389, 1980.

[9] P. G. Ciarlet and C. Mardare. Intrinsic theory of shells: Derivation from three-dimensional elasticity. *Mathematics and Mechanics of Solids*, 29(1):5–35, 2023.

[10] P. Ciarletta, G. Pozzi, and D. Riccobelli. The föppl–von kármán equations of elastic plates with initial stress. *Royal Society Open Science*, 9(5):220421, 2022.

[11] J. Dervaux, P. Ciarletta, and M. B. Amar. Morphogenesis of thin hyperelastic plates: a constitutive theory of biological growth in the föppl–von kármán limit. *Journal of the Mechanics and Physics of Solids*, 57(3):458–471, 2009.

[12] E. Efrati, E. Sharon, and R. Kupferman. Elastic theory of unconstrained non-euclidean plates. *Journal of the Mechanics and Physics of Solids*, 57(4):762–775, 2009.

[13] E. Efrati, E. Sharon, and R. Kupferman. The metric description of elasticity in residually stressed soft materials. *Soft Matter*, 9(34):8187–8197, 2013.

[14] A. Goriely. *The mathematics and mechanics of biological growth.* Springer, 2017.

[15] A. L. Gower, P. Ciarletta, and M. Destrade. Initial stress symmetry and its applications in elasticity. *Proceedings of the Royal Society A: Mathematical, Physical and Engineering Sciences*, 471(2183):20150448, 2015.

[16] A. Green and W. Zerna. *Theoretical Elasticity.* Dover Publications, 2007.

[17] W. Helfrich. Elastic properties of lipid bilayers: theory and possible experiments. *Zeitschrift für Naturforschung C*, 28(11):693–703, 1973.

[18] A. Hoger. On the residual stress possible in an elastic body with material symmetry. *Archive for Rational Mechanics and Analysis*, 88:271–289, 1985.

[19] J. D. Humphrey. Continuum biomechanics of soft biological tissues. *Proceedings of the Royal Society of London. Series A: Mathematical, Physical and Engineering Sciences*, 459(2029):3–46, 2003.

[20] W. Koiter. On the nonlinear theory of thin elastic shells. *Proceedings of the Koninklijke Nederlandse Akademie van Wetenschappen Series B Physical Sciences*, 69(1):1–54, 1966.

[21] T. Lecuit and P.-F. Lenne. Cell surface mechanics and the control of cell shape, tissue patterns, and morphogenesis. *Nature Reviews Molecular Cell Biology*, 8(8):633–644, 2007.

[22] M. Lewicka, L. Mahadevan, and M. R. Pakzad. The föppl-von kármán equations for plates with incompatible strains. *Proceedings of the Royal Society A: Mathematical, Physical and Engineering Sciences*, 467(2126):402–426, 2011.

[23] R. Lorenz. Achsensymmetrische verzerrungen in dünnwandigen hohlzylindern. *Zeitschrift des Vereines Deutscher Ingenieure*, 52(43):1706–1713, 1908.

[24] K. Marguerre. *Die Schalen mit flachem Krümmungsverlauf*. Springer, 1938.

[25] J. Merodio, R. W. Ogden, and J. Rodríguez. The influence of residual stress on finite deformation elastic response. *International Journal of Non-Linear Mechanics*, 56:43–49, 2013.

[26] P. Naghdi. Foundations of elastic shell theory. *Progress in Solid Mechanics*, IV:1–90, 1963.

[27] P. Naghdi. The theory of shells and plates. *Handbuch der Physik*, VIa/2:425–640, 1971.

[28] P. Naghdi. The theory of shells and plates. *Mechanics of Solids, Vol. IV*, pages 425–640, 1972.

[29] S. E. Naleway, J. R. Taylor, M. M. Porter, M. A. Meyers, and J. McKittrick. Structure and mechanical properties of selected protective systems in marine organisms. *Materials Science and Engineering: C*, 59:1143–1167, 2016.

[30] C. M. Nelson, M. M. VanDuijn, J. L. Inman, D. A. Fletcher, and M. J. Bissell. Emergent patterns of growth controlled by multicellular form and mechanics. *Proceedings of the National Academy of Sciences*, 102(33):11594–11599, 2005.

[31] D. Nelson. Experimental methods for determining residual stresses and strains in various biological structures. *Experimental Mechanics*, 54:695–708, 2014.

[32] V. Novozhilov. *The Strength of Materials and Theory of Elasticity in Problems*. State Publishing House for Technical-Theoretical Literature, 1951.

[33] V. Novozhilov. *Theory of Thin Shells*. P. Noordhoff, 1970.

[34] E. Reissner. The effect of transverse shear deformation on the bending of elastic plates. *Journal of Applied Mechanics*, 12:69–77, 1946.

[35] M. Shams, M. Destrade, and R. W. Ogden. Initial stresses in elastic solids: constitutive laws and acoustoelasticity. *Wave Motion*, 48(7):552–567, 2011.

[36] Z. Song and H.-H. Dai. On a consistent finite-strain shell theory based on 3-d nonlinear elasticity. *International Journal of Solids and Structures*, 97:137–149, 2016.

[37] D. Steigmann. Recent developments in the theory of nonlinearly elastic plates and shells. *Shell Structures: Theory and Applications (Vol. 2)*, pages 35–40, 2009.

[38] L. A. Taber. Biomechanics of growth, remodeling, and morphogenesis. *Applied Mechanics Reviews*, 48(8):487–545, 1995.

[39] T. Tallinen, J. Y. Chung, J. S. Biggins, and L. Mahadevan. Gyrification from constrained cortical expansion. *Proceedings of the National Academy of Sciences*, 113(44):12397–12402, 2016.

[40] S. P. Timoshenko. Einige stabilitätsprobleme der elastizitätstheorie. *Zeitschrift für Mathematik und Physik*, 58(4):337–385, 1910.

[41] V. Tvergaard and A. Needleman. A mechanical model of blastocyst hatching. *Extreme Mechanics Letters*, 42:101132, 2021.

[42] X. Zheng and J. Ren. Effects of the three-dimensional residual stresses on the mechanical properties of arterial walls. *Journal of Theoretical Biology*, 393:118–126, 2016.

MOX Technical Reports, last issues

Dipartimento di Matematica
Politecnico di Milano, Via Bonardi 9 - 20133 Milano (Italy)

03/2025 Andrini, D.; Magri, M.; Ciarletta, P.
Nonlinear morphoelastic theory of biological shallow shells with initial stress

02/2025 Corda, A.; Pagani, S.; Vergara, C.
Influence of patient-specific acute myocardial ischemia maps on arrhythmogenesis: a computational study

01/2025 Dede', L.; Parolini, N.; Quarteroni, A.; Villani, G.; Ziarelli, G.
SEIHRDV: a multi-age multi-group epidemiological model and its validation on the COVID-19 epidemics in Italy

109/2024 Liverotti, L.; Ferro, N.; Matteucci, M.; Perotto, S.
A PCA and mesh adaptation-based format for high compression of Earth Observation optical data with applications in agriculture

110/2024 Pederzoli, V.; Corti, M.; Riccobelli, D.; Antonietti, P.F.
A coupled mathematical and numerical model for protein spreading and tissue atrophy, applied to Alzheimer's disease

108/2024 Arostica, R.; Nolte, D.; Brown, A.; Gebauer, A.; Karabelas, E.; Jilberto, J.; Salvador, M.; Bucelli, M.; Piersanti, R.; Osouli, K.; Augustin, C.; Finsberg, H.; Shi, L.; Hirschvogel, M.; Pfaller, M.; Africa, P.C.; Gsell, M.; Marsden, A.; Nordsletten, D.; Regazzoni, F.; Plank, G.; Sundnes, J.; Dede’, L.; Peirlinck, M.; Vedula, V.; Wall, W.; Bertoglio, C.
A software benchmark for cardiac elastodynamics

107/2024 Chen, J.; Ballini, E.; Micheletti, S.
Active Flow Control for Bluff Body under High Reynolds Number Turbulent Flow Conditions Using Deep Reinforcement Learning

106/2024 Brunati, S.; Bucelli, M.; Piersanti, R.; Dede', L.; Vergara, C.
Coupled Eikonal problems to model cardiac reentries in Purkinje network and myocardium

105/2024 Bartsch, J.; Barakat, A.A.; Buchwald, S.; Ciaramella, G.; Volkwein, S.; Weig, E.M.
Reconstructing the system coefficients for coupled harmonic oscillators

104/2024 Cerrone, D.; Riccobelli, D.; Vitullo, P.; Ballarin, F.; Falco, J.; Acerbi, F.; Manzoni, A.; Zunino, P.; Ciarletta, P.
Patient-specific prediction of glioblastoma growth via reduced order modeling and neural

networks